Cascadability Properties of Optical 3R Regenerators Based on SOAs

Giancarlo Gavioli, *Member, IEEE*, Benn C. Thomsen, *Member, IEEE*, Vitaly Mikhailov, *Member, IEEE*, and Polina Bayvel, *Senior Member, IEEE*

***Abstract*—This paper assesses the regenerative properties of nonlinear semiconductor optical amplifier (SOA)-based optical regenerators cascaded in high-speed transmission networks. It is shown that the fundamental condition that must be ensured to maintain optimum and constant regenerative properties along a chain of concatenated nonlinear optical regenerators is that the extinction ratio at the input of each regenerator is kept constant. This condition determines an important requirement on the regenerator; signal reshaping and noise suppression must take place while performing the necessary extinction ratio enhancement to maintain cascadability. Starting from the SOA nonlinear transfer function, we derive the relationship between the extinction ratio enhancement and the noise suppression for different SOA-based gate configurations and assess their cascadability properties. This analysis is supported by experimental results of transmission with cascaded optical regeneration in a reconfigurable transmission network over transoceanic distances on standard fiber.**

***Index Terms*—All-optical switching, regeneration, semiconductor optical amplifiers (SOAs), transmission, wavelength conversion.**

I. Introduction

ALL-OPTICAL regeneration and wavelength conversion based on semiconductor optical amplifiers (SOAs) will be the key in the development of scalable and reconfigurable high-speed all-optical networks in which regenerators must compensate different amounts of signal distortion determined by routes and nodes traversed [1]. Regenerators must, therefore, be cascadable and capable of operating with different inter-regenerator spacing and of suppressing both linear and nonlinear distortions introduced in transmission and by different optical components.

In optically amplified systems, the main source of noise is the accumulation of amplified spontaneous emission (ASE) from the optical amplifiers. At high bit rates, fiber nonlinearities also significantly affect the quality of signal transmission, degrading the extinction ratio and the pulse shape [2]. Furthermore, future all-optical networks are likely to employ novel optical components such as wavelength converters, SOA optical signal amplifiers, or passive wavelength routers, which may introduce further signal distortion and extinction ratio degradation [3], [4].

Manuscript received January 17, 2007. This work was supported in part by Agilent Technologies, by the Engineering and Physical Sciences Research Council, by the EU FR-6 IP NOBEL, and by the Royal Society.

The authors are with the Optical Networks Group, Department of Electronic and Electrical Engineering, University College London, WC1E 7JE London, U.K. (e-mail: ggavioli@ee.ucl.ac.uk).

Digital Object Identifier 10.1109/JLT.2007.902116

The cascadability properties of nonlinear optoelectronic repeaters in the presence of erbium-doped fiber amplifier (EDFA) noise have been investigated theoretically to show that even a low degree of non-linearity can significantly reduce the bit-error-rate (BER) accumulation along transmission [5]. Concatenating nonlinear all-optical regenerators have also been demonstrated in loop transmission experiments (typically with constant spacing with one regenerator in the loop) to prove the feasibility of achieving ultra-long transmission distances [6]. These experiments have demonstrated that cascaded nonlinear optical regenerators can reduce the signal Q-factor degradation due to noise accumulation in transmission. However, the assessment of the noise suppression properties of a regenerator cascaded in transmission as a function of varying the noise accumulated between regenerators and the number of cascaded regenerators has not yet been presented. This assessment is critical in the design of optical networks employing optical regenerators as it can be used to determine the optimum inter-regenerator spacing and, hence, the number of regenerators required to maintain performance in a given network.

This paper investigates the reshaping properties, both noise suppression and extinction ratio enhancement, of SOA-based nonlinear optical regenerators cascaded in transmission. It is shown that there is a trade-off between the regenerator noise suppression and the extinction ratio degradation, which the regenerator can compensate for. Optical regenerators can provide a large extinction ratio gain at the cost of decreased noise suppression abilities. This ultimately determines the performance of the regenerator, its maximum tolerance to signal distortion, and, thus, its optimum position in the network.

This trade-off has also been investigated experimentally in this paper by cascading multiple optical SOA-based 3R (reamplification, reshaping, and retiming) regenerators, consisting of a wavelength conversion stage followed by an SOA-assisted interferometer, over a distance of 20 000 km, with variable inter-regenerator spacing from 150 to 750 km in a reconfigurable fiber loop test bed. Varying the inter-regenerator spacing changes the amount of noise accumulated and allows for the assessment of the cascaded regenerator noise suppression performance.

This paper is structured as follows: First, the principles of cascading nonlinear optical regenerators are summarized in Section II. In Section III, both the noise suppression and the extinction ratio enhancement properties of SOA-based optical regenerators are assessed and used to predict their performance in transmission. This paper concludes in Section IV, with the

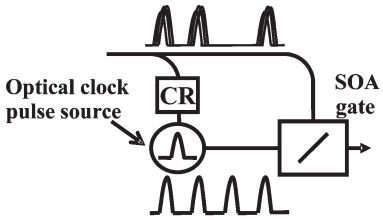

Fig. 1. Optical regeneration with a nonlinear gate.

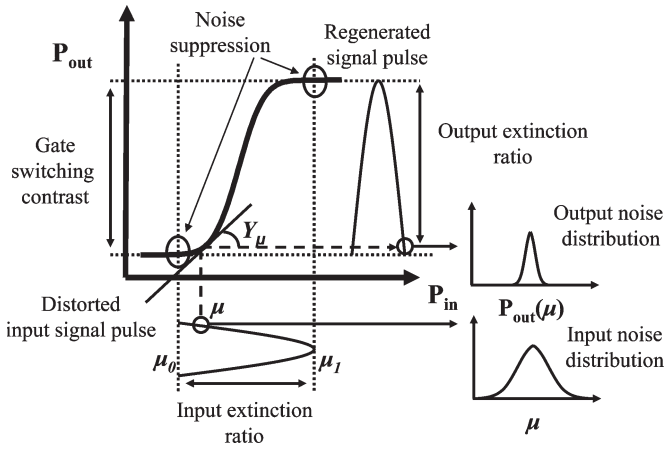

Fig. 2. Signal reshaping with a nonlinear transfer function.

results from the experimental demonstration of transmission with cascaded optical regeneration with variable inter-regenerator spacing.

II. Optical Regeneration With SOA Gates

A. Cascading Nonlinear Optical Regenerators

Fig. 1 shows the generic configuration of an optical regenerator of the type discussed in this paper [7]. The regenerator consists of an optical clock recovery (CR) unit and an optical decision circuit. The optical CR unit is responsible for the generation of a high-quality optical return-to-zero (RZ) pulse train. The decision circuit, which is an SOA-based gate in this paper, performs reshaping and retiming. Alternatively, a continuous wave signal can be used rather than the optical clock signal; however, then, only signal reshaping is performed.

The incoming and distorted input signal $(P_{\rm in})$ controls the nonlinear gate by generating a switching window which is applied to the newly generated optical clock $(P_{\rm ck})$ signal to encode the input data stream onto the new optical carrier.

The switching characteristic of an optical gate, in the absence of pattern-dependent effects, can be described by the static transfer function, which gives the relationship between the gate input and output powers. The transfer function can also be used in assessing the reshaping properties of the optical gate when this is used for optical signal regeneration.

Fig. 2 shows a general approximation of the transfer function of a bistable nonlinear gate [5].

The SOA-gate output power $(P_{\rm out})$ is given by the simple relation $P_{\rm out} = T(P_{\rm in})P_{\rm ck}$, where $T(P_{\rm in})$ is the transmittance of the gate which depends on the power of the input signal $(P_{\rm in})$. At low input power, the gate is virtually closed; at high input power, the transmittance significantly increases, and the gate is open.

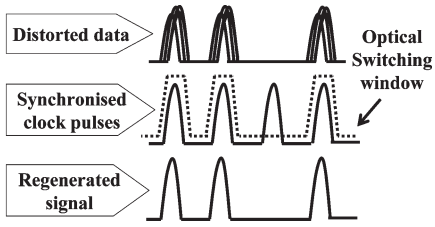

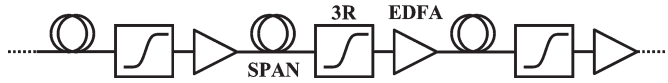

Fig. 3. Transmission system with concatenated optical regenerators.

Assessment of the reshaping properties of the optical gate involves the quantification of two fundamental parameters:

1) the signal noise suppression;
2) the regenerator extinction ratio enhancement or gain.

Here, we show that both parameters can be derived from the optical gate transfer function slope.

With reference to Fig. 2, the noise suppression performed by the optical gate transfer function at any point μ on the input pulse envelope can be estimated by approximating the regenerator transfer function around μ with a linear function with slope Y, which is defined as

$$Y_\mu = \left.\frac{dT}{dP_{\rm in}}\right|_{P_{\rm in}=\mu}. \tag{1}$$

Thus, the noise distribution function of the output signal is simply the noise distribution function of the input signal rescaled by the Y term. The standard deviation $\sigma_{\rm out}$ of the noise distribution function with mean $P_{\rm out}(\mu)$ on the output pulse envelope is given by [8]

$$\sigma_{\rm out} = Y_\mu \sigma_{\rm in} \tag{2}$$

where $\sigma_{\rm in}$ is the standard deviation of the noise distribution function with mean μ on the input pulse envelope.

As shown in (2), a nonlinear optical gate performs regeneration by noise compression, i.e., reducing the standard deviation of the input noise distribution [9]. Noise compression only occurs at the points on the transfer function where the slope Y is less than unity $|Y(P_{\rm in})| < 1$. Thus, the condition for operating the optical gate as a regenerator is that the input signal "zero" and "one" mean levels occur where the regenerator transfer function slope satisfies the above condition. The slope of the regenerator transfer function around the signal "zero" or "one" mean levels is defined here as the noise compression term $(Y_{\rm NC})$; thus, regeneration occurs when $|Y_{\rm NC}| < 1$.

The ultimate application of optical regenerators of this kind is in a transmission system, which is shown in Fig. 3, where 3R optical regenerators, which are concatenated between EDFA-amplified fiber links, are used to reduce the noise accumulation.

It has previously been shown that, assuming that each regenerator stage operates with the same noise compression term,

then, the evolution of the transmitted signal noise standard deviation σ_n after n spans can be expressed as [8]

$$\sigma_n^2 = \sigma_{n-1}^2 Y_{\mathrm{NC}}^2 + \sigma_{\mathrm{ASE}}^2 = \sigma_{\mathrm{ASE}}^2 \sum_{k=0}^{n-1} Y_{\mathrm{NC}}^{2k} \tag{3}$$

where σ_{ASE} is the standard deviation of the noise added by the optical amplifiers in the span. Thus, both the signal Q-factor and the BER accumulation in transmission can be analytically calculated simply from the noise compression term of the regenerator as in [8].

Given that the transfer function is nonlinear, then, the noise compression term is also a function of the input signal extinction ratio. Therefore, to maintain constant regenerative properties along a chain of concatenated nonlinear optical regenerators, it is necessary that the extinction ratio at the input of each regenerator is kept constant. This condition places the following important requirement on each regenerator; noise compression has to be accomplished while performing the necessary extinction ratio enhancement to maintain cascadability.

Thus, the second important parameter for optical regenerators is the extinction ratio gain ($\mathrm{ER_{gain}}$). This refers to the ability of the regenerator to improve the input signal extinction ratio and is defined as the following ratio:

$$\mathrm{ER_{gain}dB} = 10 \log \left(\frac{\mathrm{ER_{out}}}{\mathrm{ER_{in}}} \right) \tag{4}$$

where $\mathrm{ER_{in}}$ is the input signal extinction ratio (defined as $\mathrm{ER_{in}} = \mu_1/\mu_0$), and $\mathrm{ER_{out}}$ is the output extinction ratio (defined as $\mathrm{ER_{out}} = \mathrm{T}(\mu_1)/\mathrm{T}(\mu_0)$). To satisfy the condition for casacadability, $\mathrm{ER_{gain}} \geq 1$. Thus, in order to obtain optical signal regeneration in the transmission link shown in Fig. 3, each regenerator must satisfy both the noise compression and extinction ratio conditions, that is, a noise compression factor smaller than unity ($Y_{\mathrm{NC}} < 1$) and extinction ratio gain sufficient to compensate for the extinction ratio degradation caused by the transmission span.

In the next section, we consider SOA-based nonlinear optical gates and show how the regenerator noise compression term and extinction ratio gain are mathematically related to each other as well as to the SOA physical parameters.

B. SOA-Gate Transfer Function

In this section, we assess the reshaping and cascadability properties of two fundamental SOA-gates which are part of the all-optical 3R regenerator used in the transmission experiments described in the next section. The first gate, which is shown in Fig. 4(a), is based on cross-gain modulation (XGM) and is used for wavelength conversion and signal reshaping [10]. The second gate, which is shown in Fig. 4(b), is based on cross-phase modulation (XPM) and is used for wavelength conversion and 3R regeneration [11]. The regenerator studied in our experimental work makes use of both gates in order to maintain wavelength transparency. In this section, we analyze each gate individually and assess and compare their characteristics and properties.

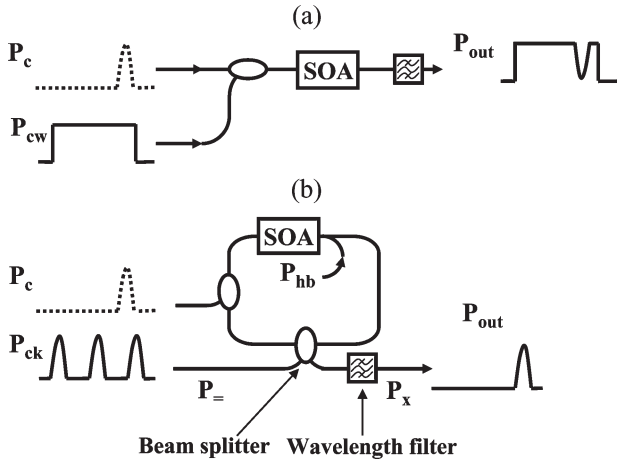

Fig. 4. All-optical gates based on (a) XGM and (b) XPM effects in SOA.

In the XGM gate, the control signal (P_{c}) is used to modulate the carrier density and, thus, the gain of an SOA and, thereby, to modulate the intensity of the continuous wave signal (P_{cw}), as shown in Fig. 4(a). The P_{cw} signal power is also used to saturate the SOA gain, shortening the gain recovery time to obtain the desired switching period [12].

If the control signal is intensity modulated with return-to-zero (RZ) or non-return-to-zero (NRZ) formats, then the XGM gate operates as a wavelength converter with 2R (reamplification and reshaping) regenerative abilities [9]. The transfer function of the XGM gate is simply the SOA gain transfer function, which can be expressed as [13]

$$G(P_{\mathrm{in}}) = \exp\left[h(P_{\mathrm{in}})\right] \tag{5}$$

$$h(P_{\mathrm{in}}) = g_0 L - P\left(\exp\left[h(P_{\mathrm{in}})\right] - 1\right) \tag{6}$$

where $P = P_{\mathrm{in}}/P_{\mathrm{sat}}$, $P_{\mathrm{in}} = P_{\mathrm{c}} + P_{\mathrm{cw}}$, P_{sat} is the saturation power given by $P_{\mathrm{sat}} = E_{\mathrm{sat}}/\tau$, where E_{sat} is the saturation energy, τ is the carrier lifetime, and $G_0 = \exp(g_0 L)$ is the amplifier small signal gain. Fig. 5(a) shows the SOA gain transfer function when P_{cw} equals zero and, thus, has no effect on the gain.

At large input optical power, the gain is saturated, and the SOA transmittance is reduced at minimum, so that the gate is closed. However, at low control powers, the gain is unsaturated, and the input signal power is amplified, so that the gate is open.

Due to the nonlinear characteristics of the transfer function, switching is accompanied by signal reshaping of the input signals. As described in the previous section, to quantify the noise compression properties of gain dependent switching, we use the slope of the $G(P_{\mathrm{in}})$ function. This is obtained by differentiating (5) with respect to the control signal power:

$$G' = \frac{dG}{dP_{\mathrm{c}}} = \frac{G(1-G)}{1+GP} \frac{1}{P_{\mathrm{sat}}}. \tag{7}$$

The magnitude of the gain transfer function slope, calculated from (7), is plotted in Fig. 5(b). The gain slope curve decreases with increasing input power, to reach values below unity at high input signal power. Referring to Fig. 2, this ensures that the noise present on the control signal "one" level is suppressed

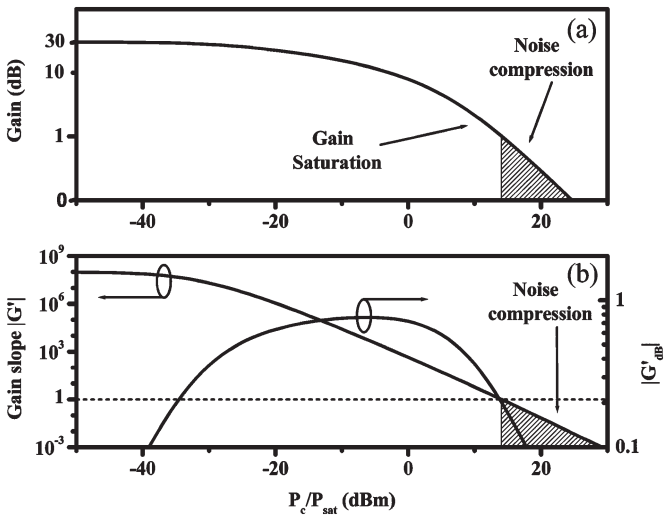

Fig. 5. (a) Gain transfer function and (b) transfer function slope with respect to the normalized control signal power for $G_0 = 30$ dB, $P_{\rm sat} = 10$ dBm, and no $P_{\rm cw}$.

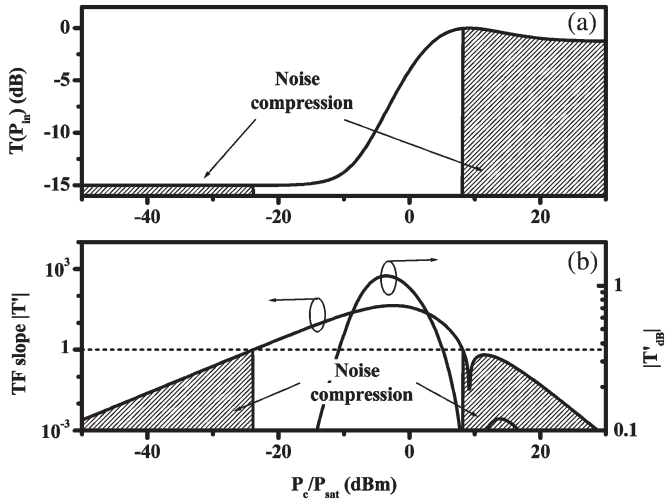

Fig. 6. (a) SOA-assisted interferometer transfer function and (b) transfer function (TF) slope with respect to the normalized control signal power, for $G_0 = 30$ dB, α-factor $= 4$, $P_{\rm sat} = 10$ dBm, $X_0 = 15$ dB, and $\varphi_{\max} = 1.3\pi$.

and not transferred on to the probe signal during the process of wavelength conversion. However, the noise associated with the "zero" level will be amplified. Thus, only limited noise suppression is performed with an XGM gate, which mainly reshapes the peak of the input signal pulse.

In order to quantify the extinction ratio enhancement provided by the nonlinear transfer function, we consider the slope of the gain transfer function expressed in decibels ($G_{\rm dB} = 10\log G$). This is defined as the derivative of $G_{\rm dB}$ with respect to the control signal power, which is also expressed in decibels, and can be calculated as

$$G'_{\rm dB} = \frac{d(10\log G)}{d(10\log P_{\rm c})} = \frac{dG}{dP_{\rm c}}\frac{P}{G}\left(1 - \frac{P_{\rm cw}}{P_{\rm in}}\right)P_{\rm sat}. \quad (8)$$

Extinction ratio enhancement can only occur when the absolute value of the $G_{\rm dB}$ slope exceeds unity. The magnitude of the $G_{\rm dB}$ slope, calculated from (8), is also plotted in Fig. 5(b) with respect to the control signal power.

The $G_{\rm dB}$ slope curve is an order of magnitude smaller around the unsaturated and transparent gain regions with respect to the values around the saturation region of the gain. However, its maximum value is less than unity, and thus, extinction ratio gain cannot be achieved.

In summary, in an XGM gate, the noise present on the control signal "one" level is compressed and not transferred onto the $P_{\rm cw}$ signal. However, extinction ratio gain cannot be achieved when switching with a gain-based nonlinearity, and thus, XGM-based gates are not cascadable.

Alternatively, optical switching with an SOA can be achieved utilizing nonlinear phase-modulation effects. This is based on the use of an SOA in an interferometer which converts the nonlinear phase shift into intensity switching [11]. Fig. 4(b) shows an SOA-assisted interferometer, which, in this case, is a Sagnac-type. Without the control signal $(P_{\rm c})$, the clock signal $(P_{\rm ck})$ is directed toward the cross output port (P_x). When the control signal is introduced into the Sagnac loop such that it only interacts with the copropagating clock signal, then a relative phase shift is obtained between the counterpropagating clock signals, which results in switching the clock signal from the cross into the bar output port $(P_=)$. For complete switching, a phase shift of π radians must be attained by setting the control signal power correspondingly. A third signal, the holding beam signal $(P_{\rm hb})$, is used to saturate the SOA gain in order to shorten the gain recovery time to the desired switching period [12].

If the control signal is intensity modulated (RZ or NRZ), then, the SOA-assisted interferometer operates as a wavelength converter with 3R regenerative abilities [14]. The SOA-assisted interferometer transfer function is given by

$$T(P_{\rm in}) = (1 - X_0)1/2\left[1 - \cos\left(\varphi(P_{\rm in}) - \theta_{\rm bias}\right)\right] + X_0 \quad (9)$$

where $P_{\rm in} = P_{\rm c} + P_{\rm hb}$ and X_0 is the interferometer switching contrast. The clock signal $(P_{\rm ck})$ is assumed not to affect the SOA gain given that $P_{\rm ck} \ll P_{\rm c}$. The term $\varphi(P_{\rm in})$ is the differential nonlinear phase shift induced in the SOA between the counterpropagating clock pulses and is defined as [13]

$$\varphi = 1/2\alpha h(P_{\rm in}). \quad (10)$$

The term $\theta_{\rm bias}$ is the interferometer phase bias and refers to the relative phase delay between the interfering components when no switching occurs.

Fig. 6(a) shows the SOA-assisted interferometer transfer function plotted using (9). The SOA gain is clamped by the holding beam signal so that the gain compression induced by the control signal only leads to a maximum phase shift of $\varphi_{\max} = 1.3\pi$ rad. The interferometer switching contrast and, thus, the output signal extinction ratio, corresponding to a π-radian shift, was chosen to be 15-dB. These values are chosen to match those of the regenerator used in the experiment presented in the next section.

Due to the sinusoidal characteristics of the transfer function, switching is accompanied by signal reshaping of the input signals. As for the XGM transfer function, the noise compression properties of an SOA-assisted interferometer can be

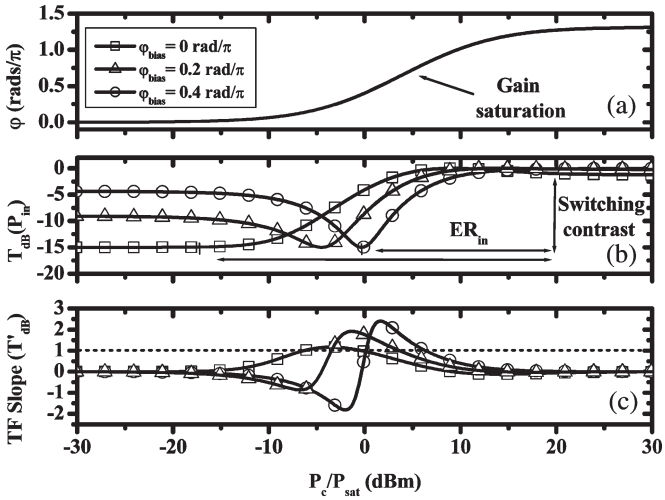

Fig. 7. (a) SOA nonlinear phase shift, (b) SOA-assisted interferometer transfer function, and (c) transfer function (TF) slope calculated for different interferometer phase bias levels for $G_0 = 30$ dB, α-factor $= 4$, $P_{\rm sat} = 10$ dBm, $X_0 = 15$ dB, and $\varphi_{\max} = 1.3\pi$.

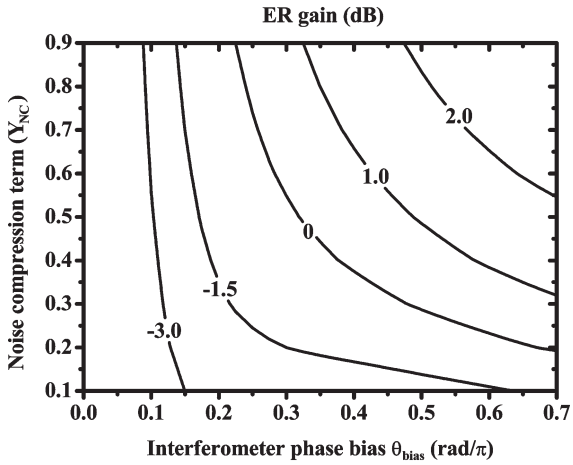

Fig. 8. SOA-assisted interferometer extinction ratio gain as a function of the interferometer phase bias and of the noise compression term for $G_0 = 30$ dB, α-factor $= 4$, $P_{\rm sat} = 10$ dBm, $X_0 = 15$ dB, and $\varphi_{\max} = 1.3\pi$.

evaluated by differentiating the interferometer equation, as expressed in (9), with respect to the control signal power. The SOA-assisted interferometer transfer function slope can be expressed as

$$T' = \frac{dT}{dP_{\rm c}} = -(1 - X_0)1/2\sin(\varphi)\frac{d\varphi}{dP_{\rm c}}. \tag{11}$$

The phase slope $d\varphi/dP_{\rm c}$ is the derivative of the SOA nonlinear phase shift with respect to the control signal power:

$$\frac{d\varphi}{dP_{\rm c}} = \left(-\frac{\alpha}{2}\right)\frac{(1-G)}{1+{\rm GP}}\frac{1}{P_{\rm sat}}. \tag{12}$$

The phase slope is indicative of the intensity-to-phase conversion efficiency of the SOA. The magnitude of the interferometer transfer function slope, which is calculated from (11), is plotted in Fig. 6(b). This is less than unity at both at high and low input powers (indicated by the shaded regions). Thus, noise compression occurs on both the "one" and "zero" signal levels, leading to complete signal reshaping.

The slope of the SOA-assisted interferometer transfer function expressed in decibels $(T'_{\rm dB})$ with respect to the control signal power, which is also in decibels, is given in (13) and also plotted in Fig. 6(b).

$$T'_{\rm dB} = \frac{d(10\log T)}{d(10\log P_{\rm c})} = \frac{dT}{dP_{\rm c}}\frac{P}{T}\left(1 - \frac{P_{\rm hb}}{P_{\rm in}}\right)P_{\rm sat}. \tag{13}$$

As shown in Fig. 6(b), the maximum value of the $T_{\rm dB}$ slope exceeds unity, which implies that an SOA-assisted interferometer can provide extinction ratio gain.

Before quantifying the extinction ratio gain, we need to assess the impact of the interferometer phase bias $(\theta_{\rm bias})$ on the transfer function $T(P_{\rm in})$, as this strongly affects the extinction ratio gain.

Fig. 7 shows how changing the phase bias, which shifts the sinusoidal transfer function of the interferometer along the nonlinear SOA phase transfer function, affects the shape of $T_{\rm dB}(P_{\rm in})$ and its slope. As the phase bias is increased, such that the interferometer operates on the saturation region of the phase transfer function, then the gate transfer function becomes sharper, and its slope maxima increases. Furthermore, the difference between the input signal mean levels $({\rm ER}_{\rm in})$ required to induce a 15 dB variation in the gate transmittance decreases as the phase bias is increased, leading to an increase in the gate extinction ratio gain which exceeds unity when ${\rm ER}_{\rm in} < X_0$.

However, when the interferometer is biased, the slope around the signal "zero" level also increases, reducing the noise-compression abilities of the regenerator. There is, thus, a trade-off in an SOA-assisted interferometer between the extinction ratio gain and the noise compression term. This trade-off, as will be shown in the next section, determines the maximum inter-regenerator spacing.

This trade-off is further investigated in Fig. 8, which shows the SOA-assisted interferometer extinction ratio gain plotted as a function of the interferometer phase bias and of the noise compression term. The extinction ratio gain is calculated from (4) for transfer functions with different phase bias values. At a given value of the phase bias, the input extinction ratio is calculated as the difference between the two input power levels at which the $T(P_{\rm in})$ slope corresponds to the $Y_{\rm NC}$ values plotted on the y-axis of Fig. 8; the corresponding output extinction ratio is calculated using (9).

Increasing the phase bias increases the achievable extinction ratio gain. However, for a given bias level, there is a trade-off between the extinction ratio gain and the noise compression. In particular, the extinction ratio gain increases with the noise compression term. This trade-off is of particular importance when transmission with cascaded regenerators is considered, where, as described earlier, both extinction ratio gain and noise compression are determinant.

Furthermore, Fig. 8 shows that with realistic values of the SOA physical parameters, the SOA-assisted interferometer configuration can provide extinction ratio gain with a noise compression term close to 0.2. This indicates that this

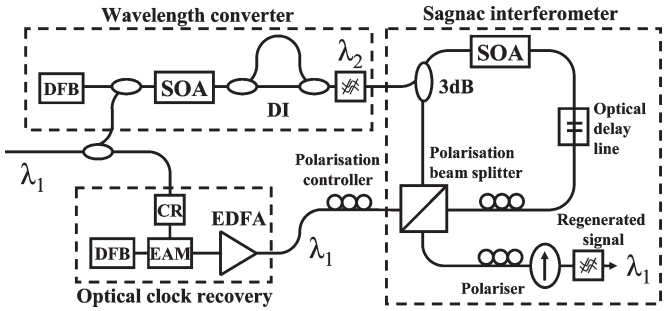

Fig. 9. 3R all-optical regenerator setup.

configuration can be cascaded, and this was experimentally investigated, as shown in the next section.

III. Experimental Investigation of Transmission With Cascaded Optical Regeneration

A. Principle of Operation and Experimental Setup

The optical 3R regenerator used in the experiments is shown in Fig. 9. It consists of an SOA-assisted fiber Sagnac interferometer operating in a polarization diversity configuration, which has been designed to take advantage of the fast polarization rotation induced by XPM and XGM in the SOA [15].

The regenerator includes a wavelength converter at the input so that the input wavelength is maintained at the output of the regenerator. The wavelength converter utilizes XGM in an SOA, followed by a delay interferometer (DI) to reshape the wavelength converted pulses [16]. The regenerator requires an optical clock to retime the input signal; this is generated using a high-Q filter-based electrical clock recovery (CR) circuit. The recovered electrical clock drives an electroabsorption modulator which generates a 10 GHz optical pulse train with 20 ps pulsewidth, synchronized to the incoming 10 Gb/s transmitted signal.

The transfer function of the interferometer is shown in Fig. 10(a). The measurements are obtained with a pump-probe setup, as in [17], and the results are fitted with (9). Fig. 10(b) shows the slope of the interferometer transfer function used to fit the experimental results in Fig. 10(a), calculated using (11). The interferometer performs noise compression on both levels providing extinction ratio gain (in excess of 2.5 dB), which was found sufficient to compensate for the extinction ratio degradation of the wavelength converter and ensure that the regenerator could cascade. The regenerator noise compression, however, is a combination of both the wavelength converter and the interferometer and, therefore, has to be measured when the regenerator is cascaded in transmission.

To investigate the reshaping and cascadability properties of the regenerator, we used a reconfigurable loop test bed, shown in Fig. 11 [18]. A 3 dB coupler is used in the loop to split the signal at the output of the transmission span into two different paths with an Acousto-Optic Modulator (AOM) in each; the first is a bypass path and the second path contains the 3R regenerator. By controlling the operating states of the AOMs in each path, the transmitted signal can be routed to the regenerator after a desired number of recirculations through

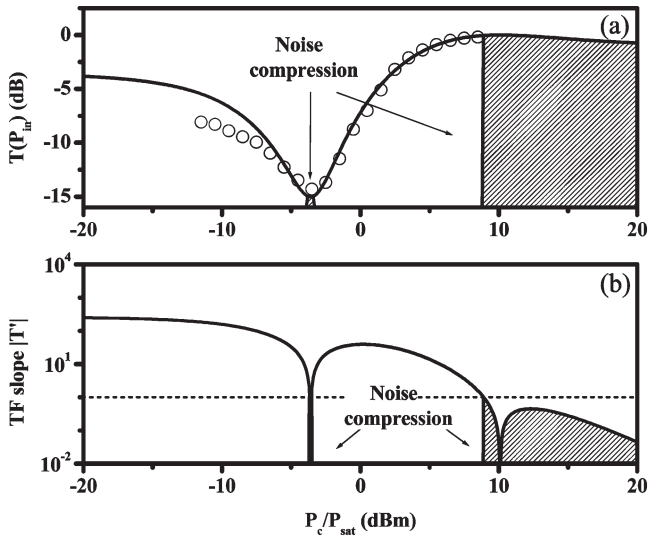

Fig. 10. (a) SOA-assisted interferometer transfer function and (b) transfer function (TF) slope measurements (o) and theoretical fits. The SOA parameters for the calculations are $G_0 = 30$ dB, α-factor $= 4$, $P_{\rm sat} = 10$ dBm, $X_0 = 15$ dB, and $\varphi_{\max} = 1.3\pi$.

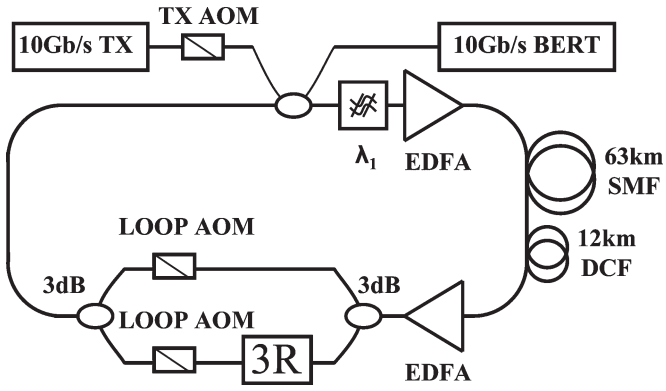

Fig. 11. Reconfigurable loop test bed used for the measurements of transmission with cascaded regeneration.

the loop transmission span. Varying the inter-regenerator spacing changes the amount of noise accumulated and allows for the assessment of the cascaded regenerator noise suppression properties.

As described in the previous sections, cascading regenerators is the optimal experimental condition to measure the regenerator noise suppression properties, because it ensures that the regenerator is providing the extinction ratio gain necessary to maintain cascadability. Furthermore, the reconfigurable loop test bed allows an assessment of the maximum spacing between regenerators and the impact of different spacing on the transmission signal Q-factor.

The loop transmission amplifier span consists of a 1 nm bandwidth optical filter and a standard Single-Mode optical Fibre link whose dispersion is fully compensated by dispersion compensating fiber (DCF), with a total length of 75 km and loss of 21 dB. An EDFA is used to compensate for the span losses and a further EDFA compensates for the losses of the reconfigurable loop components. In this configuration, the span EDFA is the dominant contributor to the optical signal-to-noise ratio (OSNR) accumulation. The transmitter generates

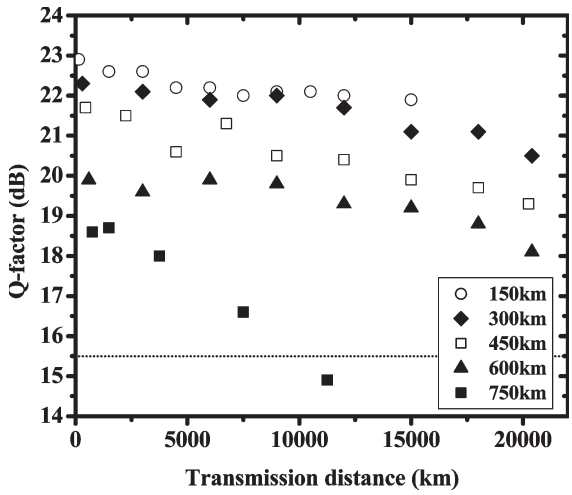

Fig. 12. Experimental Q-factor evolution with transmission distance for different inter-regenerator spacing.

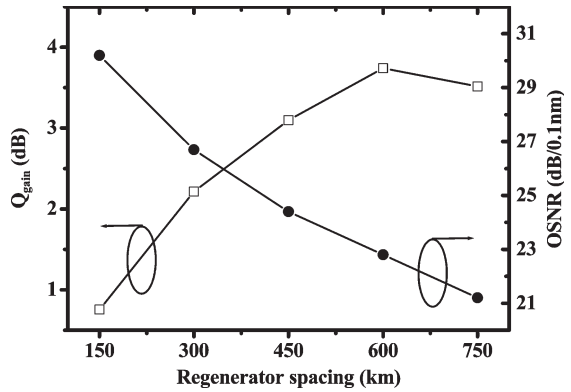

Fig. 13. Regenerator Q-gain measured after 10 000 km and OSNR at the regenerator input for different inter-regenerator spacing.

a 10 Gb/s RZ signal with 20 ps full-width at half-maximum pulses, encoded with $2^{23}-1$ Pseudo-Random Bit Sequence. The transmitter wavelength is 1550 nm, and the launch power into the fiber span was 0 dBm, ensuring that the transmission was in the linear regime. The experiments were carried out at 10 Gb/s to provide larger margins in the transmission experiments in order to focus on understanding of the principles that determine cascadability of the SOA-based regenerator.

B. Transmission Results and Discussion

Without the 3R regeneration, the maximum error-free transmission distance was OSNR limited and measured to be 2250 km. The regenerator was then placed in the loop and cascaded with different spacing over a distance fixed at 20 000 km (chosen to allow convenient BER measurement time). Fig. 12 shows the variation of the Q-factor measured as a function of transmission distance for different inter-regenerator spacing from 150 to 750 km (2–10 inter-regenerator spans).

Fig. 13 shows the OSNR at the regenerator input for the different inter-regenerator spacing. The Q measurements show that error-free transmission $(\mathrm{BER} < 1E^{-9})$ over 20 000 km with $Q^2 \geq 18$ dB can be maintained with a maximum of 600 km between regenerators and a total of 33 cascaded regenerators.

The regenerator noise suppression properties in cascaded transmission can be quantified by the parameter Q-gain, which is defined as the ratio between the Q-factor of the signal at the regenerator output and at the input, for a single regenerator within a cascaded chain. In these experiments, it was measured after a transmission distance of 10 000 km for different inter-regenerator spacing and is shown in Fig. 13. For larger inter-regenerator spacing, the regenerator operates with higher Q-gain, to compensate for the larger OSNR degradation associated with a longer span. For a spacing of up to 300 km, the Q-gain fully compensates for the span degradation, restoring the Q-factor to the value measured back-to-back at the regenerator output $(Q^2 = 22$ dB$)$.

For spacing from 150 to 600 km, the regenerator Q-gain is sufficient to suppress the accumulated noise arising from the span and to ensure that the extinction ratio condition for cascadability is maintained; however, the regenerated signal Q-factor decreases with increasing span length. The regenerator Q-gain reaches a maximum value of 3.8 dB for a spacing of 600 km. For a spacing of 750 km, the accumulation of distortion over the inter-regenerator span, measured to cause a deterioration of the signal $Q^2 = 4$ dB, exceeds the regenerator Q-factor improvement range resulting in the maximum achievable error-free transmission distance of 7500 km.

To more clearly quantify the behavior of the regenerated transmission system and to illustrate the importance of the two conditions for cascadability, we also measured the eye opening and the noise level (defined as the sum of the standard deviations of the "ones" and the "zeros") of the transmitted signal. Note that the eye opening and the noise level are simply the numerator and denominator of the Q-factor, respectively.

Fig. 14(a) shows that the eye opening (an equivalent metric to the extinction ratio) remains constant over the entire transmission distance. Before reaching a steady state, the transmitted signal eye opening oscillates slightly as it converges from the transmitter output value to the optimum value for the regenerator input.

This demonstrates that the regenerator satisfies the condition for cascadability, which is to maintain the signal extinction ratio at each regenerator input. For the case of inter-regenerator spacing equal to 10 spans (750,km) the extinction ratio gain is not sufficient to maintain cascadability, and the transmission Q-factor quickly degrades.

Fig. 14(b) shows that the noise level also does not significantly vary with transmission distance. In fact, the evolution of the signal noise standard deviation σ_n after n spans, expressed in (3), converges if Y_{NC} is a constant value between 0 and 1 to

$$\sigma^2_{n\to\infty} = \frac{\sigma^2_{\mathrm{ASE}}}{1 - Y^2_{\mathrm{NC}}} \tag{14}$$

where the n is the number of cascaded regenerators, and σ_{ASE} is the standard deviation of the noise added by the optical amplifiers in the span.

In the experimental results, the noise level initially oscillates following the variation of the transmitted signal extinction ratio, and then, it is kept constant, with small deviations which can be

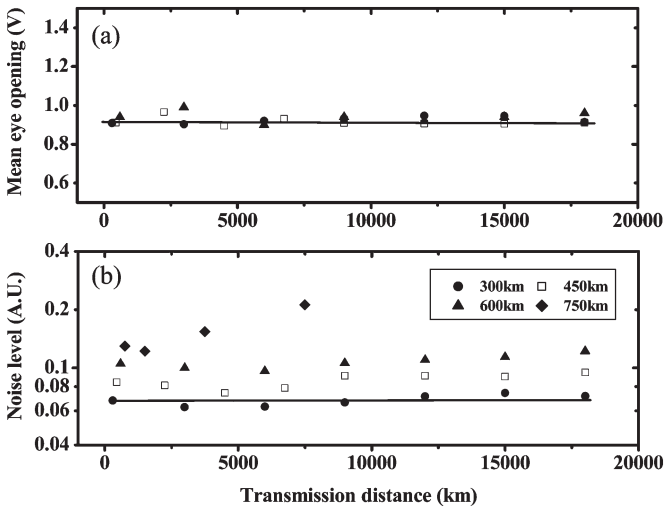

Fig. 14. (a) Mean eye opening and (b) noise level of the transmitted signal for different inter-regenerator spacing.

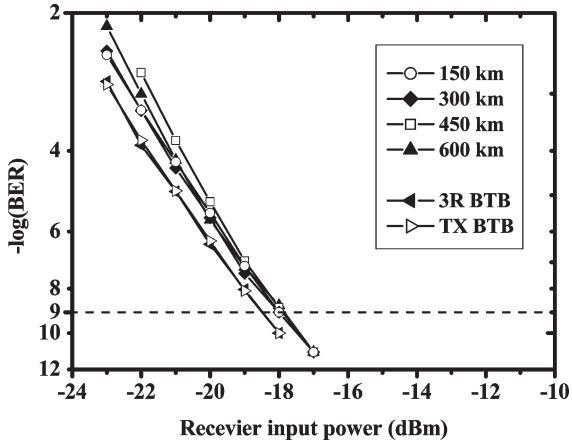

Fig. 15. BER curves measured at 20 000 km for transmission with different inter-regenerator spacing.

attributed to the accumulations with the number of recirculation of polarization dependent effects in the loop which marginally vary the signal OSNR at the span end, particularly with longer inter-regenerator spacing [19]. This demonstrates that, when the extinction ratio is maintained at the regenerator input, as shown in Fig. 14(a), then the regenerator operates with a constant noise compression term, and the noise accumulation follows (14).

It is important to note that (14) assumes that the σ_n probability density function (pdf) is Gaussian. However, as shown in [8], the tails of the σ_n pdf will increase with the number of cascaded regenerators, causing an error floor to appear in the BER, which therefore increases with distance.

In our experiments, the Q-factor is extrapolated from BER measurements of down to 1×10^{-9}, and thus, only an error floor in BER larger than 1×10^{-9} could be observed. This was the case for the measurements corresponding to transmission with inter-regenerator spacing equal to 10 spans (750 km), where both the noise level and an error floor in the BER were observed increasing with transmission distance.

Fig. 14 also shows that the noise level of the regenerated signal increases with longer inter-regenerator spacing. As shown in (14), this arises because of the increased noise accumulation between regenerators due to the longer span, while the regenerator noise compression term is largely unchanged. The noise compression term can be obtained from the measurements. Rearranging (2) for Y_{NC}, taking into account the regenerator back-to-back noise $\sigma_{\mathrm{b\text{-}b}}$

$$\sigma_{\mathrm{out}}^2 = Y_{\mathrm{NC}}^2 \sigma_{\mathrm{in}}^2 + \sigma_{\mathrm{b\text{-}b}}^2 \tag{15}$$

$$Y_{\mathrm{NC}}^2 = \frac{\sigma_{\mathrm{out}}^2 - \sigma_{\mathrm{b\text{-}b}}^2}{\sigma_{\mathrm{in}}^2} \tag{16}$$

where σ_{in} and σ_{out} are the sum of the noise standard deviation at the two signal levels of the regenerator input and output signal, respectively, and $\sigma_{\mathrm{b\text{-}b}}$ represents the noise introduced by the regenerator SOA ASE and by the optical clock EDFA and can be measured from the back-to-back regenerated signal Q-factor.

The value of Y_{NC} calculated from the noise level values experimentally measured at a distance of 10 000 for 600-km inter-regenerator spacing was found to be 0.38. This value does not change significantly with spacing. Equation (16) shows that the impact of $\sigma_{\mathrm{b\text{-}b}}$ on the regenerated signal is more significant for small input noise values. For this reason, the Q-gain plotted in Fig. 13 is smaller on shorter spacing, where the $\sigma_{\mathrm{b\text{-}b}}$ is the dominant source of noise on the output Q-factor.

Fig. 15 shows the BER curves measured after 20 000 km for different inter-regenerator spacing, showing error-free (BER $< 10^{-9}$) transmission with receiver sensitivity penalty of less than 1 dB with respect to the transmitter signal measured back-to-back. It is important to notice that the BER has increased as a function of distance proportionally to the decrease of the Q-factor, as shown in Fig. 12. However, since the Q-factor was as low as 22 dB, no sensitivity penalty could be measured at BER of 10^{-9}.

IV. Conclusion

This paper presents a theoretical and experimental investigation of the reshaping properties of SOA-based all-optical regenerators cascaded in transmission.

We found that in an SOA gate, noise compression only occurs for specific input signal extinction ratio due to the nonlinear transfer function shape. Thus, the cascadability condition for SOA gates can be reduced to a fundamental rule: Each regenerator in a chain has to perform sufficient extinction ratio enhancement to maintain the transmitted signal extinction ratio constant at each regenerator input.

We show that by deriving analytical equations for the slope of the SOA nonlinear gain and phase transfer function, the regenerative properties of an SOA optical gates can be related to the SOA physical parameters. By means of this approach, we compared the reshaping properties of both XGM- and XPM-based SOA regenerators, concluding that only XPM configurations can satisfy the condition for cascadability, which is to perform both noise suppression and extinction ratio enhancement. We also found that in an SOA-assisted interferometer,

the regenerator noise suppression is directly related to the regenerator extinction ratio enhancement. For this reason, we conclude that, when characterizing the regenerator reshaping properties, it is necessary to measure its noise compression, while this operates with the extinction ratio gain necessary to maintain cascadability.

The reshaping properties of an SOA-assisted interferometer regenerator cascaded in a transmission were also measured utilizing a reconfigurable fiber recirculating loop to show that the cascaded regenerator can perform Q-factor improvement of up to 3.8 dB. We have also experimentally demonstrated that when the extinction ratio is maintained at the regenerator input, then the regenerator operates with a constant noise compression term, which, in our experiment, was measured to be 0.38. This was sufficient to allow 10 Gb/s transmission over 20 000 km with optical regenerators cascaded every 600 km.

ACKNOWLEDGMENT

The authors would like to thank C. R. Doerr and M. Zirngibl (Bell Labs, Lucent Technologies) for the loan of the DI interferometer, C. Tombling and Kamelian Ltd. for the loan of the SOAs, and C. Weber and S. Savory for useful comments. G. Gavioli would like to thank the IEEE Lasers and Electro-Optics Society for the award of a Postgraduate Fellowship in 2005.

REFERENCES

[1] M. Dueser and P. Bayvel, "Analysis of a dynamically wavelength-routed optical burst switched network architecture," *J. Lightw. Technol.*, vol. 20, no. 4, pp. 574–585, Apr. 2002.

[2] V. Mikhailov, R. I. Killey, S. Appathurai, and P. Bayvel, "Investigation of intrachannel nonlinear distortion in 40 Gb/s transmission over standard fibre," *Fiber Integr. Opt.*, vol. 22, no. 3, pp. 189–195, Jun. 2003.

[3] Y. Kim, H. Jang, Y. Kim, J. Lee, D. Jang, and J. Jeong, "Transmission performance of 10 Gbps 1550-nm transmitters using semiconductor optical amplifiers as booster amplifiers," *J. Lightw. Technol.*, vol. 21, no. 2, pp. 476–481, Feb. 2003.

[4] B. Puttnam, M. Dueser, and P. Bayvel, "Experimental investigation of the signal degradation in WDM transmission through coherent crosstalk caused by a fast tunable SG-DBR laser," presented at the Optical Fiber Commun. Conf. (OFC), Anaheim, CA, Mar. 6–11, 2005, Paper JWA30.

[5] P. Ohlén and E. Berglind, "Noise accumulation and BER estimates in concatenated nonlinear optoelectronic repeaters," *IEEE Photon. Technol. Lett.*, vol. 9, no. 10, pp. 1479–1481, Oct. 2003.

[6] B. Lavigne, E. Balmefrezol, P. Brindel, B. Dagens, R. Brenot, L. Pierre, J. L. Moncelet, D. de la Grandiére, J. C. Remy, J. C. Bouley, B. Thedrez, and O. Leclerc, "Low input power all-optical 3R regenerator based on SOA devices for 42.66 Gbit/s ULH WDM RZ transmissions with 23 dB span loss and all-EDFA amplification," presented at the Optical Fiber Commun. Conf. (OFC), Atlanta, GA, Mar. 22–28, 2003, Paper PD15-1.

[7] O. Leclerc, B. Lavigne, E. Balmefrezol, P. Brindel, L. Pierre, D. Rouvillain, and F. Seguineau, "Optical regeneration at 40 Gb/s and beyond," *J. Lightw. Technol.*, vol. 21, no. 11, pp. 2779–2790, Nov. 2003.

[8] J. Mork, F. Ohman, and S. Bischoff, "Analytical expression for the bit error rate of cascaded all-optical regenerators," *IEEE Photon. Technol. Lett.*, vol. 15, no. 10, pp. 1479–1481, Oct. 2003.

[9] D. Wolfson, S. L. Danielsen, H. N. Poulsen, P. B. Hansen, and K. E. Stubkjaer, "Experimental and theoretical investigation of the regenerative capabilities of electrooptic and all-optical interferometric wavelength converters," *IEEE Photon. Technol. Lett.*, vol. 10, no. 10, pp. 1413–1415, Oct. 1998.

[10] S. L. Danielsen, C. Joergensen, M. Vaa, B. Mikkelsen, K. E. Stubkjaer, P. Doussiere, and F. L. Pommerau, "Bit error rate assessment of 40 Gb/s all-optical polarisation independent wavelength converter," *Electron. Lett.*, vol. 32, no. 18, pp. 1688–1690, Aug. 1996.

[11] M. Eiselt, W. Pieper, and H. G. Weber, "Decision gate for all-optical data retiming using a semiconductor laser amplifier in a loop mirror configuration," *Electron. Lett.*, vol. 29, no. 1, p. 107, Jan. 1993.

[12] R. Manning and D. Davies, "Three-wavelength device for all-optical signal processing," *Opt. Lett.*, vol. 19, no. 12, pp. 889–891, Jun. 1994.

[13] G. P. Agrawal and N. A. Olsson, "Self-phase modulation and spectral broadening of optical pulses in semiconductor laser amplifiers," *IEEE J. Quantum Electron.*, vol. 25, no. 11, pp. 2297–2306, Nov. 1989.

[14] D. A. O. Davies, A. D. Ellis, and G. Sherlock, "Regenerative 20 Gb/s wavelength conversion and demultiplexing using a semiconductor laser amplifier nonlinear loop mirror," *Electron. Lett.*, vol. 31, no. 12, pp. 1000–10 018, Jun. 1995.

[15] G. Gavioli and P. Bayvel, "Novel 3R regenerator based on polarisation switching in a semiconductor optical amplifier-assisted fiber Sagnac interferometer," *IEEE Photon. Technol. Lett.*, vol. 15, no. 9, pp. 1261–1263, Sep. 2003.

[16] J. Leuthold, B. Mikkelsen, R. E. Behringer, G. Raybon, C. H. Joyner, and P. A. Besse, "Novel 3R regenerator based on semiconductor optical amplifier delayed-interference configuration," *IEEE Photon. Technol. Lett.*, vol. 13, no. 8, pp. 860–862, Aug. 2001.

[17] W. Idler, K. Daub, G. Laube, M. Schilling, P. Wiedemann, K. Dutting, M. Klenk, E. Lach, and K. Wunstel, "10 Gb/s wavelength conversion with integrated multiquantum-well-based 3-port Mach–Zehnder interferometer," *IEEE Photon. Technol. Lett.*, vol. 8, no. 9, pp. 1163–1165, Sep. 1996.

[18] G. Gavioli, V. Mikhailov, B. Thomsen, and P. Bayvel, "Investigation of transmission with cascaded all-optical 3R regenerators and variable inter- regenerator spacing," *Electron. Lett.*, vol. 41, no. 3, pp. 146–148, Feb. 2005.

[19] M. Nissov, J. X. Cai, A. N. Pilipetskii, Y. Cai, C. R. Davidson, A. Lucero, and N. S. Bergano, "Q-factor fluctuations in long distance circulating loop transmission experiments," presented at the Optical Fiber Commun. Conf. (OFC), Los Angeles, CA, Feb. 22–27, 2004, Paper MF6.

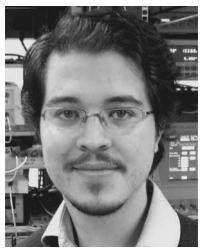

Giancarlo Gavioli (M'02) was born in Vimercate, Italy, in 1976. He received the B.Eng. degree in electronic engineering from Oxford Brookes University, Oxford, U.K., in 1999 and the MRes degree in telecommunications and the Ph.D. degree, focusing on the area of optical processing devices for multiwavelength optical networks, nonlinear effects in semiconductor optical amplifier, and high-bit-rate transmission systems, from University College London (UCL), London, U.K., in 2000 and 2006, respectively.

Since 2006, he has been a Research Fellow, working with the Optical Networks Group, UCL, on all-optical processing and high-bit-rate transmission for future all-optical networks.

Dr. Gavioli was recently awarded a Leverhulme Research Fellowship to work on 160-Gb/s all-optical devices. In 2005, he was awarded the IEEE Lasers and Electro-Optics Society Postgraduate Fellowship.

Benn C. Thomsen (M'07) received the B.Tech. degree (first class honors) in optoelectronics, the M.Sc. degree (with distinction), and the Ph.D. degree in physics from The University of Auckland, Auckland, New Zealand. His Ph.D. research involved the development and characterization of short optical pulse sources suitable for high-capacity optical communication systems and the development of nonlinear switching technologies for high-speed all-optical demultiplexing in optical-time-division-multiplexing systems.

He then joined the Optoelectronics Research Centre, Southampton University, Southampton, U.K., as a Research Fellow in 2002, where he carried our research on ultrashort optical pulse generation and characterization, optical packet switching based on optically coded labels, and all-optical pulse processing. Since 2004, he has been with the Optical Networks Group, University College London, London, U.K. His current research focuses on all-optical regeneration and physical layer implementation of dynamic optical networks. He has authored/coauthored over 50 papers in journals and conferences in the area of optical communication and optical pulse characterization.

Dr. Thomsen was recently awarded an Engineering and Physical Sciences Research Council Advanced Research Fellowship.

Vitaly Mikhailov (S'00–M'02) was born in Leningrad, Russia, formerly the U.S.S.R., in 1973. He received the M.Sc. degree from Leningrad Electrical Engineering Institute, Saint Petersburg, Russia, in 1996. Since 1997, he has been working toward the Ph.D. degree at the Optical Networks Group, Department of Electronic and Electrical Engineering, University College London (UCL), London, U.K.

Currently, he is a Research Fellow with the Optical Networks Group, UCL, where his fields of interest are nonlinear fiber effects in high-speed wavelength-division-multiplexing transmission systems and the design of novel transmitters, demultiplexers, and routers for wavelength-routed optical networks.

Mr. Mikhailov was the recipient of the IEEE Lasers and Electro-Optics Society postgraduate fellowship award in 2000.

Polina Bayvel (SM'00) received the B.Sc.(Eng.) and Ph.D. degrees in electronic and electrical engineering from the University College London (UCL), London, U.K., in 1986 and 1990, respectively. In her Ph.D. work, she specialized in nonlinear fiber optics and their applications.

Following a Royal Society postdoctoral exchange fellowship in 1990 with the Fiber Optics Laboratory, General Physics Institute (U.S.S.R. Academy of Sciences), Moscow, Russia, she worked as a Principal Systems Engineer with STC Submarine Systems, Ltd., Greenwich, U.K., and Nortel Networks, Harlow, U.K., where she worked on the design and planning of high-speed optical transmission networks. During 1993–2003, she held a Royal Society University Research Fellowship at UCL, during which she started and built up the Optical Networks research group at UCL, with research interests in the areas of high-speed wavelength-division-multiplexing transmission and wavelength routing, static and dynamic optical network architectures, nonlinear optics and optical processing, including switching and regeneration, and associated devices. She is currently a Professor of optical communications and networks and leads the Optical Networks Group, UCL. Currently, she is a Vice-Dean of the Faculty of Engineering Sciences, UCL, with responsibilities for research. More recently, she has also been working in the area of quantum computation and processing techniques and algorithms. She has authored/coauthored over 200 refereed journals and conference papers.

Dr. Bayvel was the recipient of the 2002 Institute of Physics Paterson Medal and Prize for her contributions to theoretical and experimental research in the fundamental aspects of nonlinear fiber optics and their understanding and application in optical communications systems and networks. In 2005, she was the Technical Programme Committee Chair of the 31st European Conference on Optical Communications, Glasgow, U.K. She is a Fellow of the Royal Academy of Engineering, a Fellow of the Institution of Electrical Engineers, and a Fellow of the Institute of Physics.